Electronic Supporting Information for

Supramolecular assemblies based on Fe_8L_{12} cubic metal-organic cages: synergistic adsorption and spin-crossover properties

Hui-Shu Lu,‡[a] Wang-Kang Han,‡[a] Xiaodong Yan,[a] Ya-Xin Xu,[a] Hai-Xia Zhang,[a] Tao Li,[a] Yu Gong,[a] Qing-Tao Hu,[a] and Zhi-Guo Gu*[a,b]

[a]*The Key Laboratory of Synthetic and Biological Colloids, Ministry of Education, School of Chemical and Material Engineering, Jiangnan University, Wuxi 214122, P.R.China*
[b]*International Joint Research Center for Photoresponsive Molecules and Materials, School of Chemical and Material Engineering, Jiangnan University, Wuxi 214122, China*

‡ These authors contributed equally.

E-mail: zhiguogu@jiangnan.edu.cn

Table of Contents

1. Experimental Section

All reagents and solvents were reagent grade, purchased from commercial sources and used without further purification.

Infrared spectra were measured with a Nicolet 6700 FT–IR spectrophotometer with ATR attachment in the range of 500-4000 cm^{-1} region. Nuclear magnetic resonance (NMR) spectra were recorded on AVANCE III (400 MHz) instrument at 298 K using standard Bruker software, and chemical shifts were reported in parts per milion (ppm) downfield from tetramethylsilane. The electrospray ionization mass spectrometry (ESI-MS) spectra were recorded using an LCQ fleet APT/SSQ-710 ESI-MS spectrometer (Finnigan MAT). Element analyses were conducted on elementar corporation vario ELIII analyzer. UV/vis absorbance spectra were collected on Shimadzu UV-2101 PC scanning spectrophotometer. The thermogravimetric analysis (TGA) were carried out by using TGA/1100SF thermograbinetric analyzer with a heating rate of 15 $°C\cdot min^{-1}$ from 25 to 900 °C under N_2 atmosphere. Power X-ray Diffraction (PXRD) data on the crystalline were collected on a D8 Advance X-ray diffractometer (Bruker AXS Germany) with Cu Kα radiation in a 2θ range from 3° to 50° at the speed of 2° min^{-1} at room temperature. Low-pressure (up to 1 bar) gas adsorption isotherms (N_2) were measured on a Micrometrics ASAP 2020 MP Surface Area and Porosity Analyzer. Regrettably, the BET studies have failed maybe due to the high test pressure, which caused the flexible assemblies to become tightly packed. Variable-temperature magnetic susceptibilities on crystalline samples were performed on a Quantum Design MPMS-XL-7 SQUID magnetometer with an applied magnetic field of 1000 Oe over the temperature range of 2-400 K. The molar susceptibilities were corrected for diamagnetic contributions using Pascal's constants and the increment method. Samples were restrained with petroleum jelly to prevent decomposing of the crystallites.

2. Synthesis

2.1 Synthesis of 1, 3-bis(2-bromoethoxy)benzene

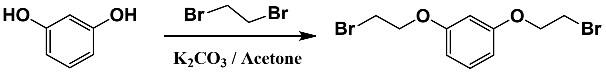

A mixture of resorcinol (3.303 g, 30 mmol) and anhydrous potassium carbonate (11.056 g, 80 mmol) in a 250 mL three round bottom flask containing 80 mL acetone was stirred under nitrogen atmosphere at 60 °C for 2 hours. Then, excess 1,2-dibromoethane (40 mL) was added, the reaction mixture was further stirred for 24 h and filtered. The filtrate was evaporated with a rotary evaporator to removed 1,2-dibromoethane and solvent. The residue was dissolved in 100 mL chloroform, and washed with sodium hydroxide solution (3×50mL), water (2×50 mL). And the extracting solution was dried over anhydrous $MgSO_4$. After $CHCl_3$ was removed and dried under vacuum in 40 °C to give 1, 3-bis(2-bromoethoxy)benzene as a yellowish-brown solid powder (Yield: 41 %). ESI-MS (m/z): 323.92. Anal. Calcd for $C_{10}H_{12}Br_2O_2$: C, 37.07; H, 3.73; Br, 49.32. Found: C, 37.20; H, 3.84; Br, 49.18; ATR-FTIR (ν cm^{-1}): 3092, 2972, 2931, 1584, 1490, 1453, 1274, 1191, 1156, 1067, 1025, 853, 756, 684, 615. ^1H NMR (400 MHz: $CDCl_3$, δ ppm): 7.22 (t, $1H^1$), 6.57 (d, $2H^2$), 6.52 (t, $1H^3$), 4.28-4.32 (t, $4H^4$), 3.64-3.68 (t, $4H^5$).

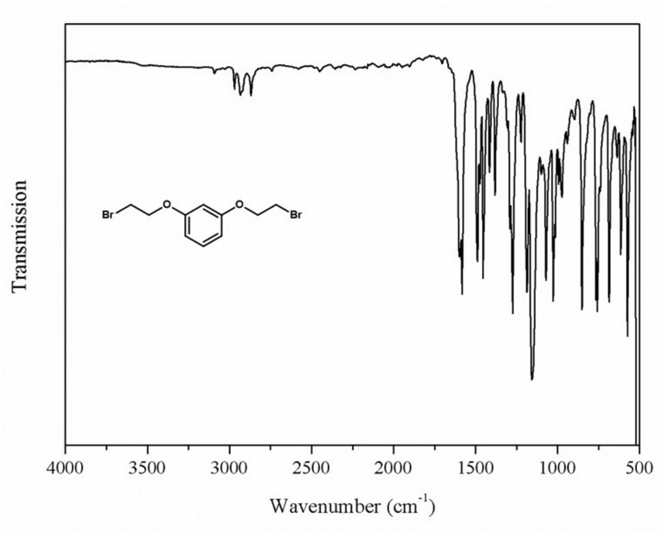

Figure. S1. ATR FT-IR spectrum of 1, 3-bis(2-bromoethoxy)benzene.

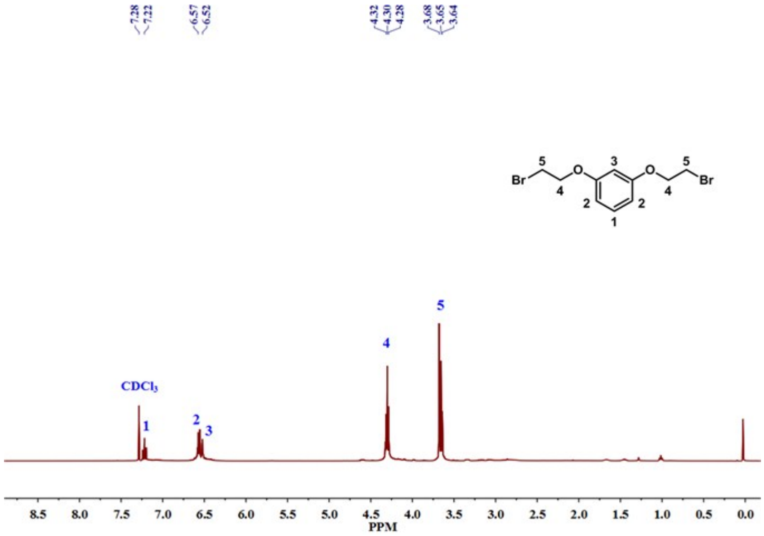

Figure. S2. ^{1}H NMR spectrum of 1, 3-bis(2-bromoethoxy)benzene.

2.2 Synthesis of 3,5-bis(2-bromoethoxy)methylbenzene

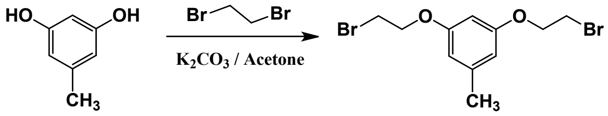

3,5-bis(2-bromoethoxy)methylbenzene was prepared in a manner analogous to that of 1, 3-bis(2-bromoethoxy)benzene except that 5-methylbenzene-1,3-diol (3.724 g, 30 mmol) was used instead of resorcinol (Yield: 37 %). ESI-MS (m/z): 337.93. Anal. Calcd for $C_{11}H_{14}Br_2O_2$: C, 39.08; H, 4.17; Br, 47.28. Found: C, 39.20; H, 4.02; Br, 47.40; ATR-FTIR (v cm^{-1}): 3033, 2973, 2916, 1585, 1490, 1448, 1419, 1381, 1322, 1275, 1153, 1072, 838, 799, 683, 574. ^{1}H NMR (400 MHz: $CDCl_3$, δ ppm): 6.39 (d, 2H^2), 6.33 (t, 1H^3), 4.26-4.30 (t, 4H^4), 3.63-3.66 (t, 4H^5), 2.32 (s, 3H^1).

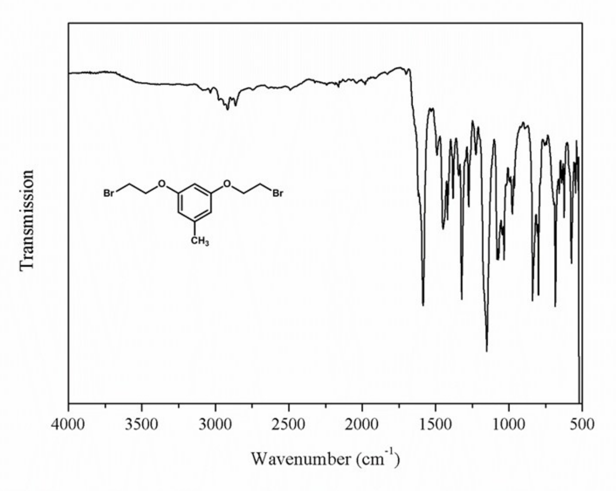

Figure. S3. ATR FT-IR spectrum of 3,5-bis(2-bromoethoxy)methylbenzene.

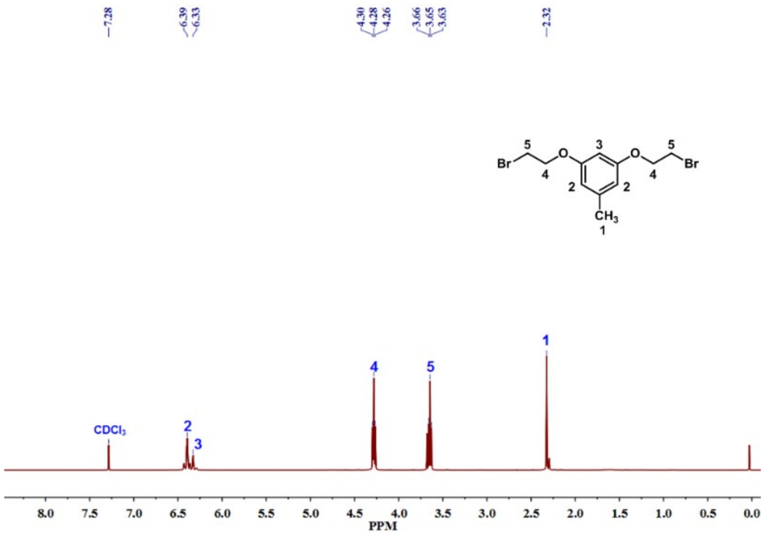

Figure. S4. ^{1}H NMR spectrum of 3,5-bis(2-bromoethoxy)methylbenzene.

2.3 Synthesis of 1,3-bis(2-(1-(imidazole-2-carbaldehyde))bromoethoxy)benzene

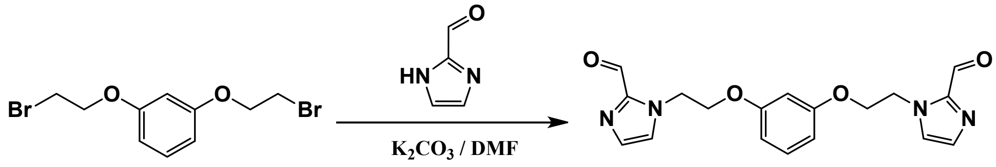

Imidazole-2-carboxaldehyde (1.35 g, 14 mmol), 1, 3-bis(2-bromoethoxy)benzene (1.62 g, 5 mmol), and potassium carbonate (1.38 g, 10 mmol) were added to a 100 mL flask containing 30 mL DMF in nitrogen atmosphere. The reaction mixture was stirred at 50 °C for 3 days and then filtered. The filtrate was extracted with water (30 mL) and ethyl acetate (50 mL), collecting the organic phase, washed with saturated aqueous solution of potassium chloride, dried with anhydrous magnesium sulfate, removed the solvent on a rotary evaporator and dried under vacuum in 40 °C for 12 h to give the desired product as yellow crystals (Yield: 48 %). ESI-MS (m/z): 354.13. Anal. Calcd for $C_{18}H_{18}N_4O_4$: C, 61.01; H, 5.12; N, 15.81. Found: C, 61.16; H, 5.21; N, 15.66; ATR-FTIR (ν cm^{-1}): 3087, 2931, 2842, 1677, 1591, 1493, 1473, 1412, 1335, 1286, 1265, 1246, 1184, 1152, 1081, 1049, 826, 767, 682. ^1H NMR (400 MHz: CD3CN, δ ppm): 9.74 (s, $2H^1$), 7.46 (s, $2H^2$), 7.25 (s, $2H^3$), 7.13-7.17 (t, $1H^8$), 6.47-6.50 (m, $2H^6$), 6.40-6.42 (t, $1H^7$), 4.75-4.78 (t, $4H^4$), 4.28-4.28 (t, $4H^5$).

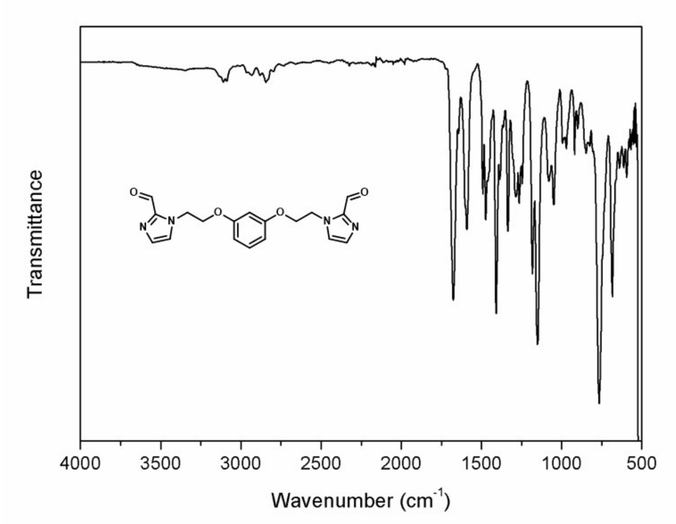

Figure. S5. ATR FT-IR spectrum of 1,3-bis(2-(1-(imidazole-2-carbaldehyde))bromoethoxy)benzene.

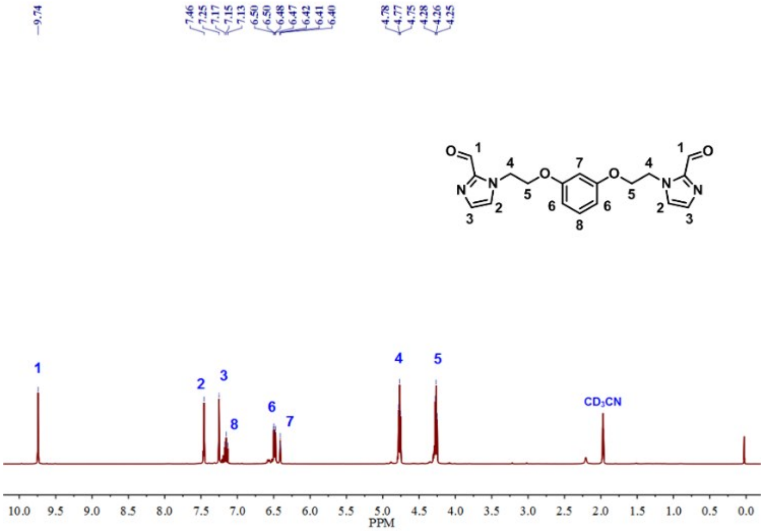

Figure. S6. ^{1}H NMR spectrum of 1,3-bis(2-(1-(imidazole-2-carbaldehyde))bromoethoxy)benzene.

2.4 Synthesis of 3,5-bis(2-(1-(imidazole-2-carbaldehyde))bromoethoxy)toluene

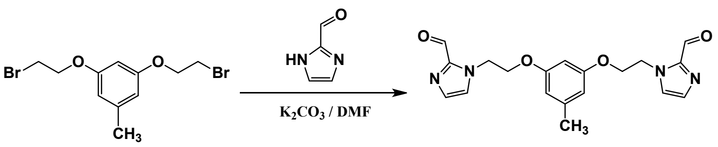

Imidazole-2-carboxaldehyde (1.35 g, 14 mmol), 3, 5-bis(2-bromoethoxy)methylbenzene (1.69 g, 5 mmol), and potassium carbonate (1.38 g, 10 mmol) were added to a 100 mL flask containing 30 mL DMF in nitrogen atmosphere. The reaction mixture was stirred at 50 °C for 3 days and then filtered. The filtrate was extracted with water (30 mL) and ethyl acetate (50 mL), collecting the organic phase, washed with saturated aqueous solution of potassium chloride, dried with anhydrous magnesium sulfate, removed the solvent on a rotary evaporator and dried under vacuum in 40 °C to give the desired product as yellow crystals (Yield: 53 %). ESI-MS (m/z): 368.15. Anal. Calcd for $C_{19}H_{20}N_4O_4$: C, 61.95; H, 5.47; N, 15.21. Found: C, 61.84; H, 5.34; N, 15.30; ATR-FTIR (ν cm^{-1}): 3104, 2925, 2843, 1673, 1591, 1474, 1408, 1356, 1295, 1248, 1151, 1073, 829, 768, 695. ^{1}H NMR (400 MHz: CD_3CN, δ ppm): 9.74 (s, 2H^1), 7.45 (s, 2H^2), 7.25 (s, 2H^3), 6.33 (s, 2H^6), 6.21 (s, 1H^7), 4.74-4.76 (t, 4H^4), 4.22-4.25 (t, 4H^5), 2.23 (s, 3H^8).

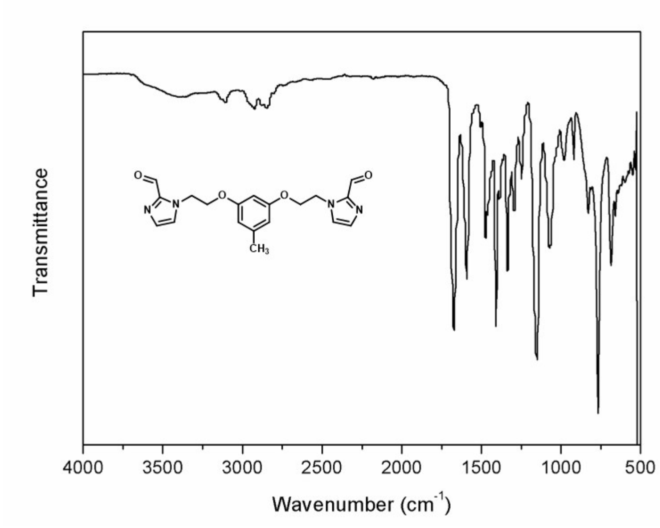

Figure. S7. ATR FT-IR spectrum of 3,5-bis(2-(1-(imidazole-2-carbaldehyde))bromoethoxy)toluene.

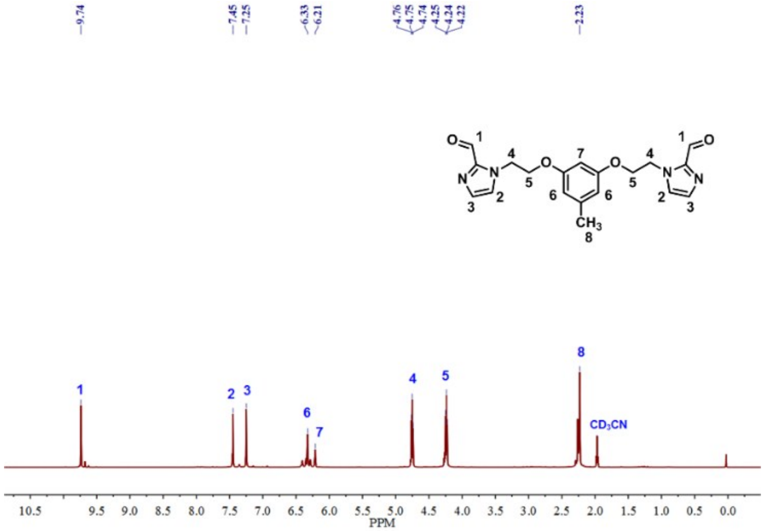

Figure. S8. ^{1}H NMR spectrum of 3,5-bis(2-(1-(imidazole-2-carbaldehyde))bromoethoxy)toluene.

2.5 Synthesis of 1

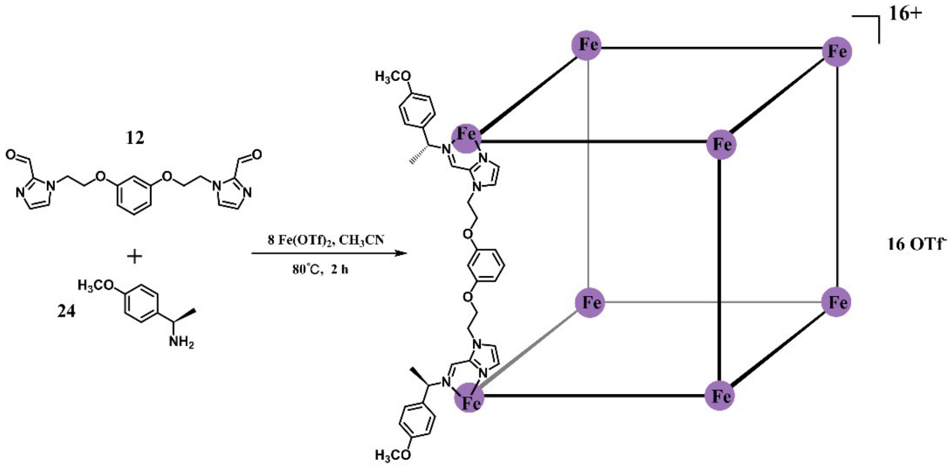

1,3-bis(2-(1-(imidazole-2-carbaldehyde))bromoethoxy)benzene (0.0708 g, 0.2 mmol), *R*-1-(4-methoxyphenyl)ethan-1-amine (0.0605 g, 0.4 mmol) and Fe(OTf)$_2$ (0.0472 g, 0.133 mmol) were added to a flask with 20 mL of acetonitrile in N_2 atmosphere. The solution was stirred and heated at 80 °C for 2 h, cooled to room temperature. Then, the resulting purple solution was filtered. Next, the filtrate was transferred to five separate test tubes (1.5 × 10 cm), and then the test tubes were placed in the jar (500 mL) containing 200 mL diethyl ether. Cage **1** was precipitated as dark purple crystals through slow diffusion of diethyl ether into the filtrate at room temperature. Yield: 48 %. Anal. Calcd for $C_{448}H_{528}F_{48}Fe_8N_{72}O_{96}S_{16}$: C, 52.09; H, 5.15; N, 9.76. Found: C, 52.41; H, 5.52; N, 9.23; For **1** (with solvent molecules), found: C, 55.35; H, 6.75; N, 8.16; ATR-FTIR (ν cm^{-1}): 3122, 2974, 2936, 1605, 1585, 1512, 1442, 1242, 1146, 1028, 832, 764, 635.

2.6 Synthesis of 2

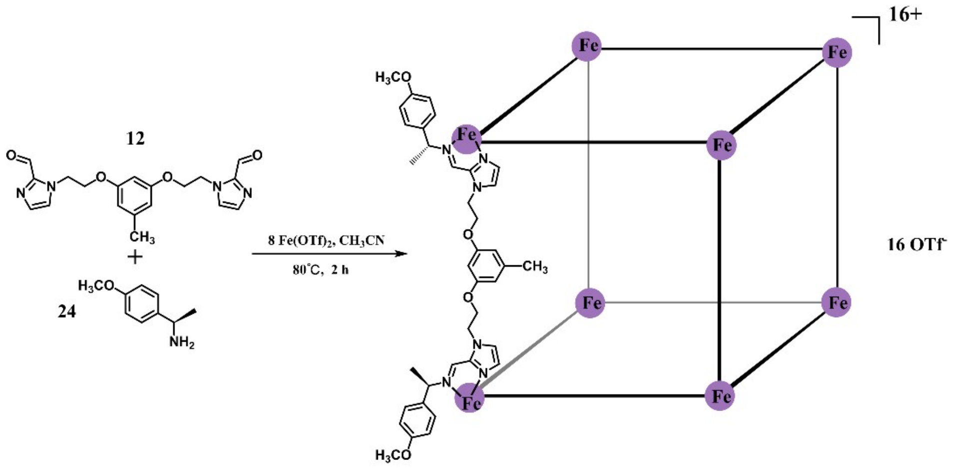

3,5-bis(2-(1-(imidazole-2-carbaldehyde))bromoethoxy)toluene (0.0737g, 0.2 mmol), *R*-1-(4-methoxyphenyl)ethan-1-amine (0.0605 g, 0.4 mmol) and Fe(OTf)$_2$ (0.0472 g, 0.133 mmol) were added to a flask with 20 mL of acetonitrile in nitrogen atmosphere. The solution was stirred and heated at 80 °C for 2 h, cooled to room temperature. Then, the resulting purple solution was filtered. Next, the filtrate was transferred to five separate test tubes (1.5 × 10 cm), and then the test tubes were placed in the jar (500 mL) containing 200 mL diethyl ether. Cage **2** was precipitated as dark purple crystals through slow diffusion of diethyl ether into the filtrate at room temperature. Yield: 53 %. Anal. Calcd for $C_{460}H_{552}F_{48}Fe_8N_{72}O_{96}S_{16}$: C, 52.63; H, 5.30; N, 9.61. Found: C, 53.04; H, 5.86; N, 9.08; For **2** (with solvent molecules), found: C, 55.64; H, 6.91; N, 8.78; ATR-FTIR (ν cm^{-1}): 3123, 2970, 2935, 1597, 1514, 1244, 1147, 1028, 831, 770, 634.

3. TGA, IR, UV-Vis and ESI-MS characterization of 1-2

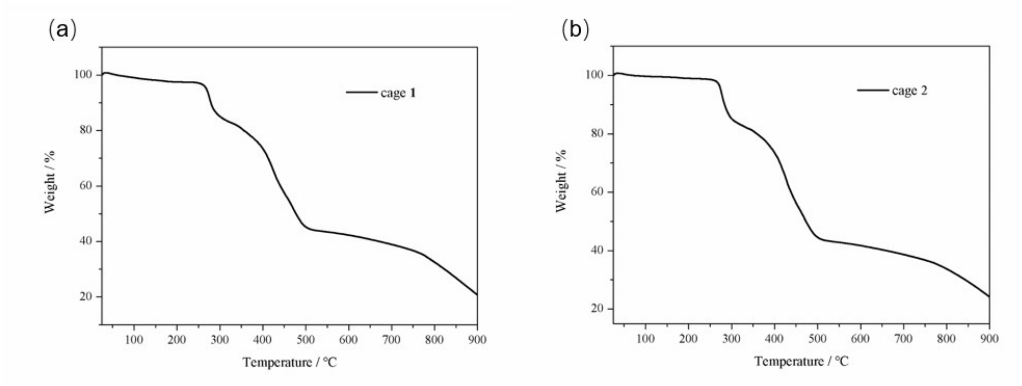

Figure. S9. Thermogravimetric analysis (TGA) curves of (a) **1** and (b) **2**.

The weight of **1** and **2** were nearly a constant following the increasing temperature until 280 °C for **1**, 290 °C for **2**, and then the complex started to decompose. Further heated to 900 °C, there were approximate 22 and 23 percent of weight residual for these two cages, which possibly corresponded to the iron oxides.

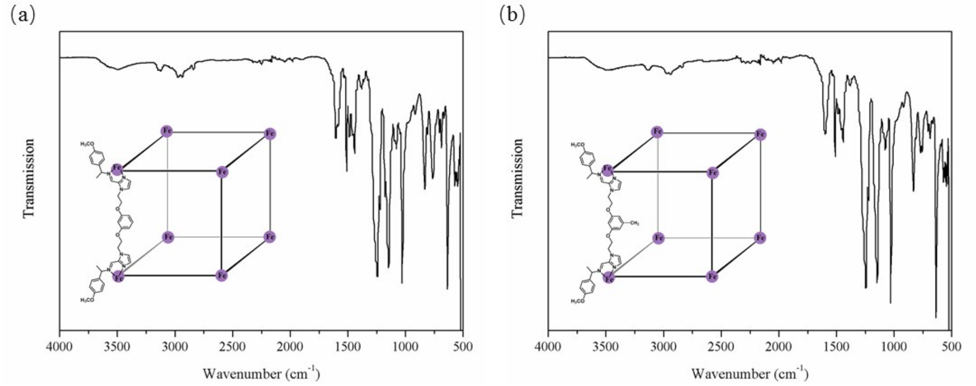

Figure. S10. IR spectra of (a) **1** and (b) **2**.

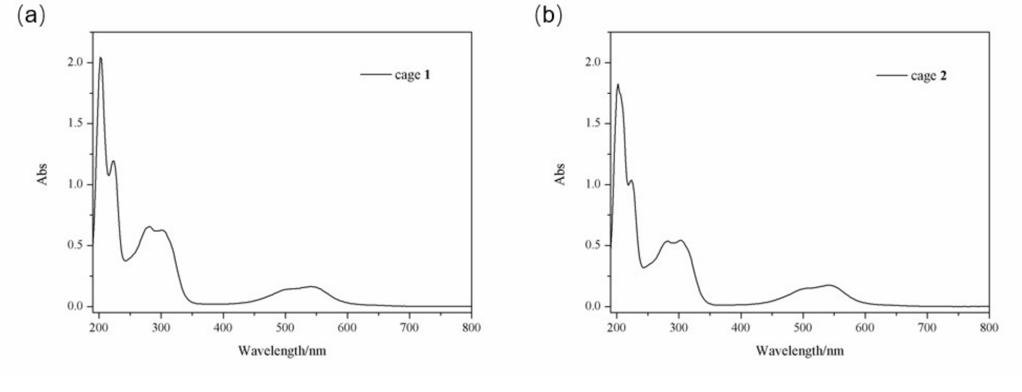

Figure. S11. UV-Visible spectra of (a) **1** and (b) **2** in MeCN (10^{-5} M).

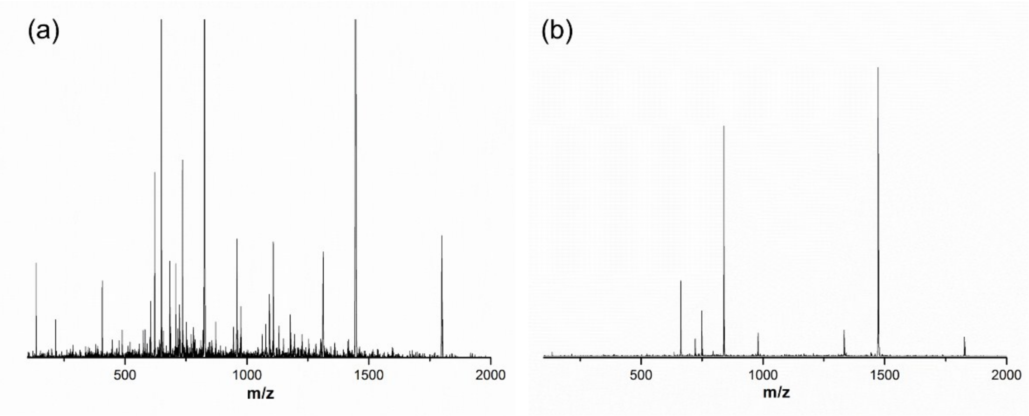

Figure. S12. ESI-MS spectra of (a) **1**, (b) **2**.

4. X-ray structures of 2

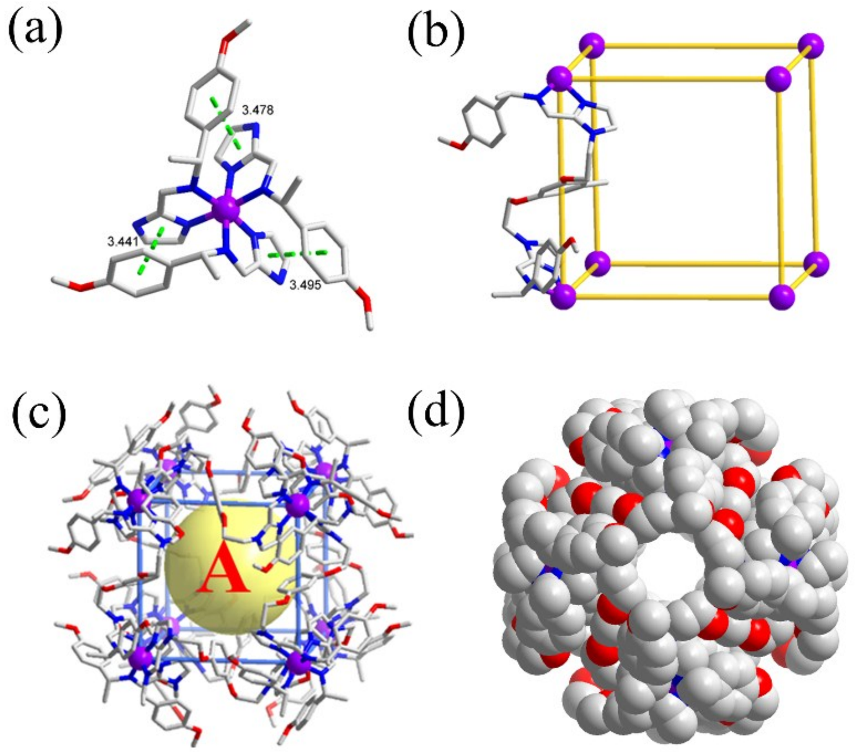

Figure. S13. (a) C_3-symmetric iron coordinate vertex (Green broken lines represent π–π interactions), (b) the cubic cage structure, (c) X-ray crystal structures, (d) the space-filling view of cage **2**. All H atoms, anions and solvents have been removed for clarity. (C: Grey; N: blue; O: red; Fe: purple).

The average Fe–N bond length of **2** was 1.972 Å. The Fe-Fe spacing was in the range of 11.712-11.730 Å for **2**. As the methyl groups on the bridging group benzene ring in the middle of the ligand all point to the inner cavity of the metal organic cage **2**, the range of the inner cavity of the cage becomes smaller, so the volume of the cavity A inside the cubic cage is about 659 Å^3.

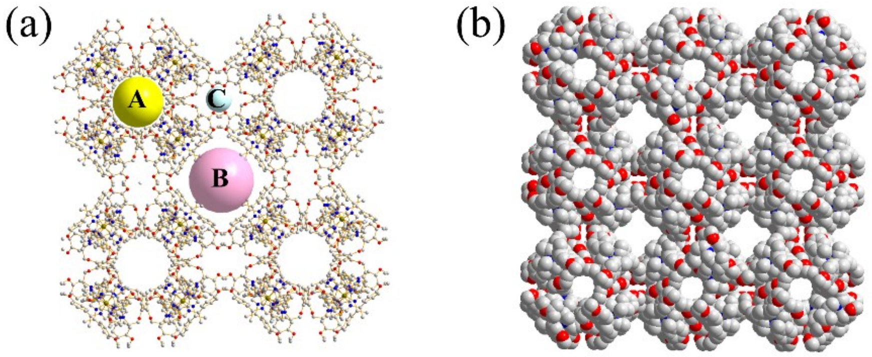

Figure. S14. Crystal packing diagrams of **2**.

5. The experiment of host-guest behaviors.

5.1 The experiment of host-guest behaviors about I_2

A volumetric flask was used to accurately prepare iodine cyclohexane solution with a concentration of 2.0×10^{-3} mol·L^{-1}. 25 mg crystal was added in the experimental flask and 3 mL iodine cyclohexane solution with a concentration of 2.0×10^{-3} mol·L^{-1} was added. The ultraviolet absorption spectrometers were used to measure the ultraviolet absorption of the residual solution under 25 °C water bath constant temperature. The formula used to calculate the iodine uptake of **1** and **2** is as follows: $m_1 = \frac{n_0 \times M_0}{n_1}$, where m_1 was the iodine adsorption, n_0 (mol) was iodine amount, M_0 was molecular weight of iodine, and n_1 (mol) was amount of **1** or **2**.

5.2 The experiment of host-guest behaviors about TTF

A volumetric flask was used to accurately prepare TTF cyclohexane solution with a concentration of 2.0×10^{-3} mol·L^{-1}. 25 mg crystal was added in the experimental flask and 3 mL TTF cyclohexane solution with a concentration of 2.0×10^{-3} mol·L^{-1} was added. The ultraviolet absorption spectrometers were used to measure the ultraviolet absorption of the residual solution under 25 °C water bath constant temperature.

5.3 The experiment of synergistic host-guest behaviors about I_2 and TTF

25 mg crystal was weighed in the experimental flask, and 3 mL iodine cyclohexane solution with a concentration of 2.0×10^{-3} mol·L^{-1} was added. The solution was balanced at a constant temperature of 25 °C water bath for at least 24 h. After the iodine was completely absorbed by the crystal (the solution changed from purple to colorless), the solution in the bottle was replaced with 3 mL TTF cyclohexane solution with a concentration of 2.0×10^{-3} mol·L^{-1}. The ultraviolet absorption spectrograph was used to measure the ultraviolet absorption of the remaining solution under 25 °C water bath constant temperature for different times. The formula used to calculate the TTF uptake

of **1** and **2** is as follows: $m_1 = \frac{n_0 \times M_0}{n_1}$, where m_1 was the TTF adsorption, n_0 (mol) was TTF amount, M_0 was relative molecular weight of TTF, n_1 (mol) was amount of **1** or **2**. Anal. Calcd for I_2/TTF⊂**1**, found: C, 53.48; H, 5.65; N, 8.36; For I_2/TTF⊂**2**, found: C, 53.62; H, 6.53; N, 8.58.

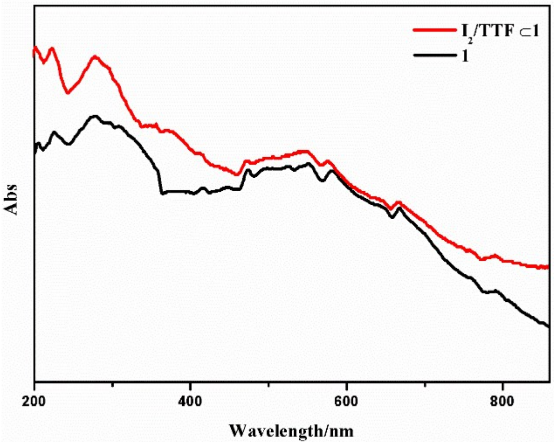

Figure. S15. Solid state UV-vis-NIR absorption spectra of I_2/TTF⊂**1** and **1**.

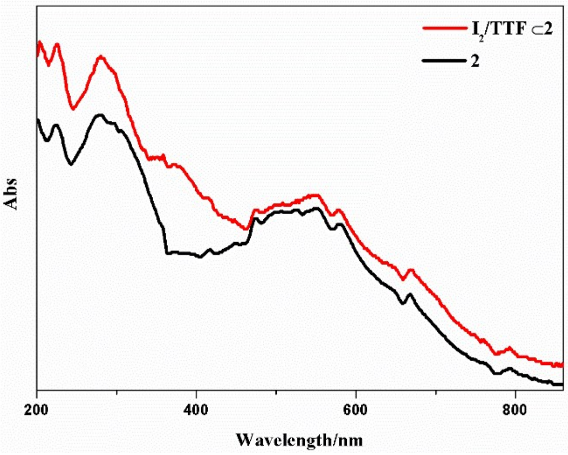

Figure. S16. Solid state UV-vis-NIR absorption spectra of I_2/TTF⊂**2** and **2**.

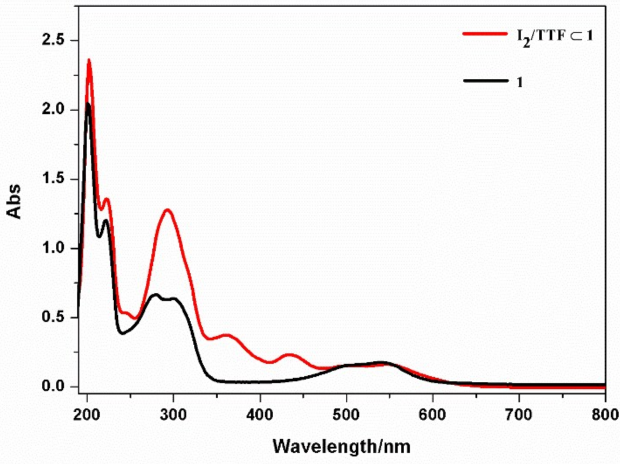

Figure. S17. UV-Visible spectra of I_2/TTF⊂**1** and **1** in MeCN (10^{-5} M).

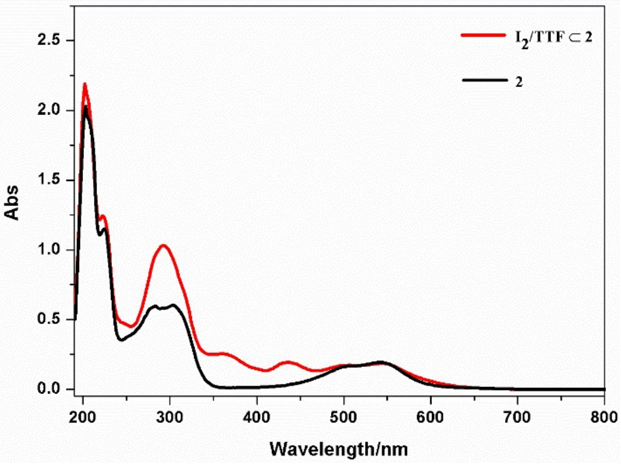

Figure. S18. UV-Visible spectra of I_2/TTF⊂**2** and **2** in MeCN (10^{-5} M).

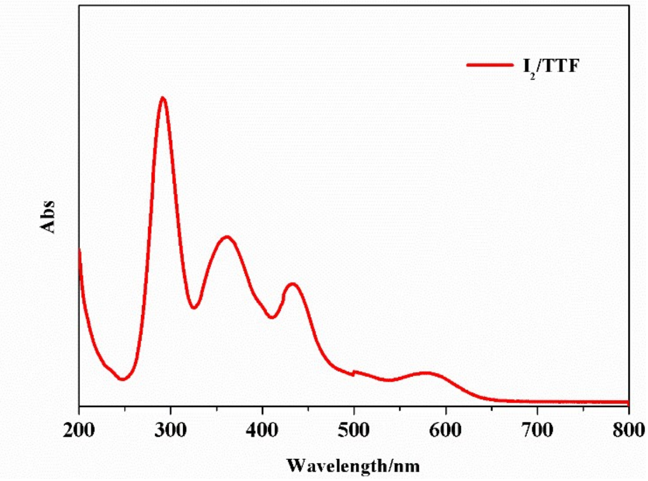

Figure. S19. UV-Visible spectra of I_2/TTF in MeCN (10^{-5} M).

To confirm the synergistic adsorption of I_2 and TTF, solid state UV-vis-NIR absorption spectra were measured (Fig. S15-S16). The peak around 380 nm for TTF cation was found in I_2/TTF⊂**1** and I_2/TTF⊂**2**. In addition, after dissolving I_2/TTF⊂**1** and I_2/TTF⊂**2** in solution, the appearance of characteristic peaks for I_2 and TTF around 380 nm and 440 nm also proved the synergistic adsorption (Fig. S17-S19).

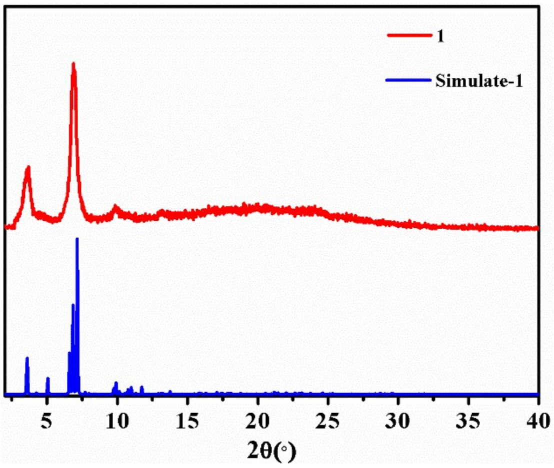

Figure. S20. PXRD spectra of **1** and simulate-**1**.

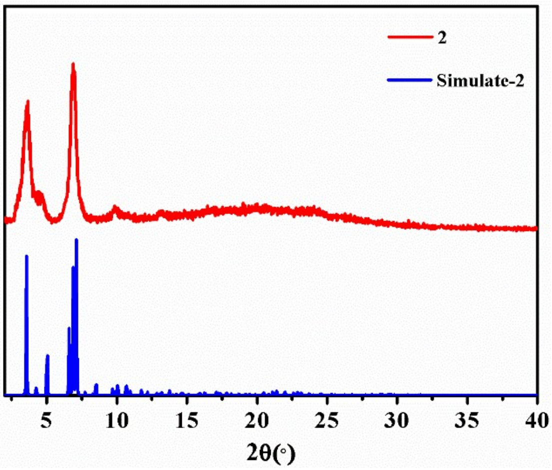

Figure. S21. PXRD spectra of **2** and simulate-**2**.

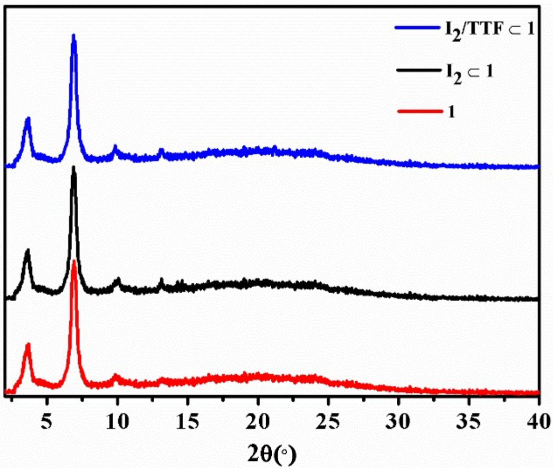

Figure. S22. PXRD spectra of **1**, I_2⊂**1** and I_2/TTF⊂**1**.

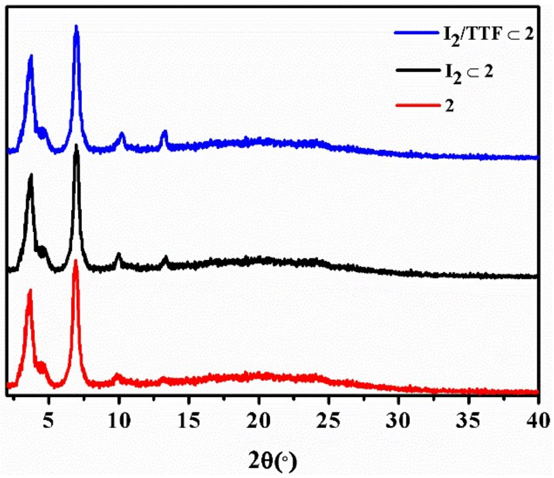

Figure. S23. PXRD spectra of **2**, I_2⊂**2** and I_2/TTF⊂**2**.

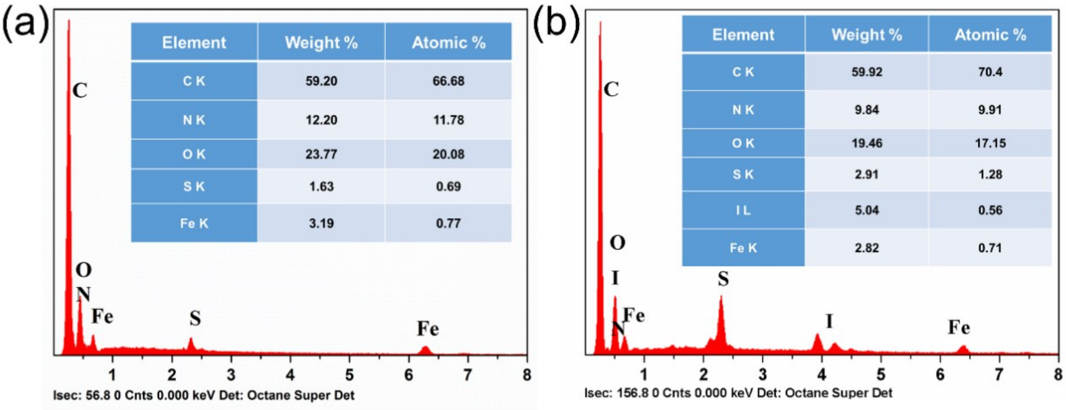

(a)

Element	Weight %	Atomic %
C K	59.20	66.68
N K	12.20	11.78
O K	23.77	20.08
S K	1.63	0.69
Fe K	3.19	0.77

(b)

Element	Weight %	Atomic %
C K	59.92	70.4
N K	9.84	9.91
O K	19.46	17.15
S K	2.91	1.28
I L	5.04	0.56
Fe K	2.82	0.71

Figure. S24. EDX spectra of (a) **1** and (b) I_2/TTF⊂**1**.

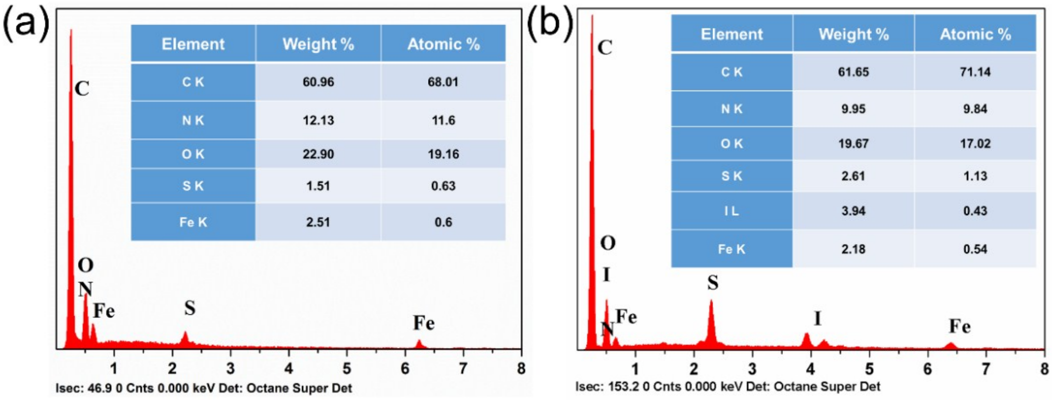

(a)

Element	Weight %	Atomic %
C K	60.96	68.01
N K	12.13	11.6
O K	22.90	19.16
S K	1.51	0.63
Fe K	2.51	0.6

(b)

Element	Weight %	Atomic %
C K	61.65	71.14
N K	9.95	9.84
O K	19.67	17.02
S K	2.61	1.13
I L	3.94	0.43
Fe K	2.18	0.54

Figure. S25. EDX spectra of (a) **2** and (b) I_2/TTF⊂**2**.

According to the EDX analysis, the absorption quantity of I_2 is about 510 mg/mmol for **1**, 490 mg/mmol for **2**, and the absorption quantity of TTF is about 430 mg/mmol for **1**, 390 mg/mmol for **2**.

5.4 The experiment of synergistic host-guest behaviors about I_2/TTF

A volumetric flask was used to accurately prepare I_2/TTF THF solution with a concentration of 2.0 × 10^{-3} mol·L^{-1}. 25 mg crystal was added in the flask, and 3 mL I_2/TTF THF solution with a concentration of 2.0 × 10^{-3} mol·L^{-1} was added. A ultraviolet absorption spectrometer was used to measure the ultraviolet absorption of the residual solution under 25 °C water bath at constant temperature.

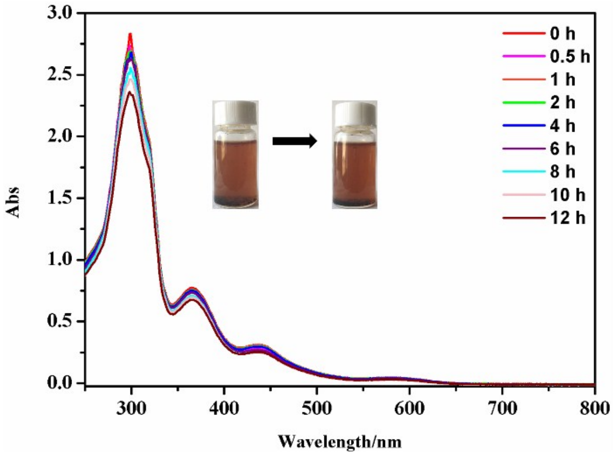

Figure. S26. The UV/vis spectra of I_2/TTF solution (2.0 × 10^{-3} mol·L^{-1}, 3 mL) was adsorbed by **1**.

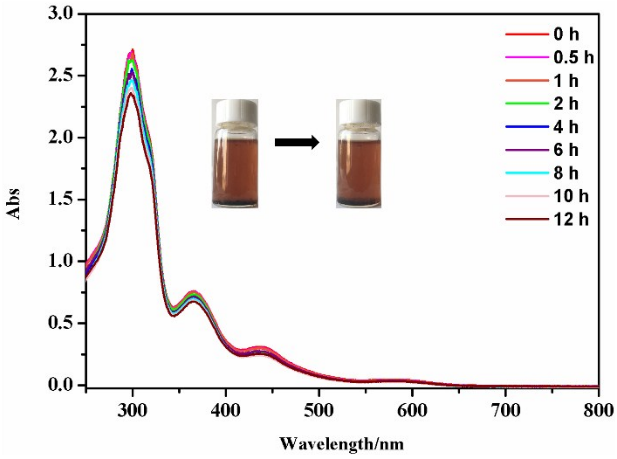

Figure. S27. The UV/vis spectra of I_2/TTF solution (2.0 × 10^{-3} mol·L^{-1}, 3 mL) was adsorbed by **2**.

After adding **1** and **2** crystals to the I_2/TTF solution, no obvious change in the solution colour and the intensity of the characteristic absorption peaks was observed, indicating that TTF cation can hardly be adsorbed by **1** and **2**.

6. X-ray Crystallography

The crystal structures were determined on a Siemens (Bruker) SMART CCD diffractometer using monochromated Mo $K\alpha$ radiation (λ = 0.71073 Å). Cell parameters were retrieved using SMART software and refined using SAINT[1] on all observed reflections. The highly redundant data sets were reduced using SAINT[1] and corrected for Lorentz and polarization effects. Absorption corrections were applied using SADABS[2] supplied by Bruker. Structures were solved by direct methods using the 2014 version of SHELXL program .[3] All of the non-hydrogen atoms except the anions were refined with anisotropic thermal displacement coefficients. Hydrogen atoms of organic ligands were located geometrically and refined in a riding model, whereas those of solvent molecules were not treated during the structural refinements. Disorder was modeled using standard crystallographic methods including constraints, restraints and rigid bodies where necessary. The crystals of cage **1** and **2** decayed rapidly out of solvent, despite rapid handling and long exposure times, the data collected were less than ideal quality. Reflecting the instability of the crystals, there were a large area of smeared electron density present in the lattice. Despite many attempts to model this region of disorder as a combination of solvent molecules no reasonable fit could be found and accordingly these regions were treated with the SQUEEZE[4] function of PLATON[5]. For cage **1**, all OTf¯ anions no reasonable could be found. And 8 1-(4-methoxy-phenyl)ethylamine groups are disordered. For cage **2**, twelve OTf¯ anions no reasonable could be found, and 16 1-(4-methoxy-phenyl)ethylamine groups are disordered. Final crystallographic data for cages **1**-**2** are listed in Table S1, and the selected bond distances [Å] and angles [°] are listed in Table S2.

Table S1 Summary of crystallographic data for **1** and **2**

	1	**2**
Formula	$C_{432}H_{480}Fe_8N_{72}O_{48}$	$C_{444}H_{504}Fe_8N_{72}O_{48}$
Fw	7895.65	8660.24
T (K)	172(2)	173(2)
λ (Å)	0.71073	0.71073
Crystal system	Tetragonal	Tetragonal
Space group	$I422$	$I422$
a (Å)	34.9266(13)	35.1488(12)
b (Å)	34.9266(13)	35.1488(12)
c (Å)	25.815(2)	25.6895(18)
α (0)	90	90
β (0)	90	90
γ (0)	90	90
V (Å^3)	31491(3)	31738(3)
Z	2	2
D_{calc} (Mg/m^3)	0.833	0.906
μ (mm^{-1})	0.230	0.249
F(000)	8336	9112
θ (0)	2.7-23.3	2.9-23.4
Index ranges	$-38 <= h <= 26$ $-38 <= k <= 38$ $-28 <= l <= 22$	$-35 <= h <= 38$ $-39 <= k <= 39$ $-27 <= l <= 28$
Reflections	34627	54857
GOF (F^2)	1.186	1.198
$R_1{}^a$, $wR_2{}^b$($I>2\sigma(I)$)	0.0847, 0.2043	0.1143, 0.2729
$R_1{}^a$, $wR_2{}^b$(all data)	0.2090, 0.2615	0.2017, 0.3492

$R_1{}^a = \Sigma||F_o| - |F_c||/\Sigma F_o|$. $wR_2{}^b = [\Sigma w(F_o{}^2 - F_c{}^2)^2/\Sigma w(F_o{}^2)]^{1/2}$

Table S2 Selected bond lengths [Å] and angles [°] for **1** and **2**

1			
Fe1-N1A	1.880(11)	Fe1-N3C	1.933(11)
Fe1-N1C	1.907(11)	Fe1-N1B^{a}	1.947(11)
Fe1-N3A	1.911(11)	Fe1-N3B^{a}	1.967(11)
N1A-Fe1-N1C	92.1(5)	N1Ba-Fe1-N1C	91.8(5)
N1A-Fe1-N3A	79.5(5)	N3A-Fe1-N3C	94.9(4)
N1A-Fe1-N3C	91.3(4)	N1Ba-Fe1-N3A	93.3(5)
N1A-Fe1-N1B^{a}	93.3(5)	N3A-Fe1-N3B^{a}	98.1(4)
N1A-Fe1-N3B^{a}	171.8(5)	N1Ba-Fe1-N3C	171.2(5)
N1C-Fe1-N3A	170.3(5)	N3Ba-Fe1-N3C	96.8(5)
N1C-Fe1-N3C	80.5(4)	N1Ba-Fe1-N3B^{a}	79.0(5)
N1C-Fe1-N3B^{a}	90.9(5)		
2			
Fe1-N1A	1.948(12)	Fe1-N3B	1.981(12)
Fe1-N1B	1.979(11)	Fe1-N1C^{a}	1.981(12)
Fe1-N3A	1.994(14)	Fe1-N3C^{a}	1.950(14)
N1A-Fe1-N1B	93.7(5)	N1B-Fe1-N3C^{a}	91.1(5)
N1A-Fe1-N3A	79.4(5)	N3A-Fe1-N3B	96.7(6)
N1A-Fe1-N3B	90.7(5)	N1Ca-Fe1-N3A	90.3(6)
N1A-Fe1-N1C^{a}	90.4(5)	N3A-Fe1-N3C^{a}	96.2(5)
N1A-Fe1-N3C^{a}	171.5(5)	N1Ca-Fe1-N3B	173.0(6)
N1B-Fe1-N3A	172.3(5)	N3B-Fe1-N3C^{a}	97.1(5)
N1B-Fe1-N3B	79.8(6)	N1Ca-Fe1-N3C^{a}	82.3(5)
N1B-Fe1-N1C^{a}	93.2(6)		

7. References

[1] *SAINT-Plus*, version 6.02; Bruker Analytical X-ray System: Madison, WI, 1999.

[2] Sheldrick, G. M. *SADABS An empirical absorption correction program*, Bruker Analytical X-ray Systems: Madison, WI, 1996.

[3] Sheldrick, G. M. (2014) SHELXL-2014/7: program for the solution of crystal structures. University of Göttingen, Göttingen.

[4] P. van der Sluis and A. L. Spek, *Acta Crystallogr., Sect. A: Found. Crystallogr.*, 1990, **46**, 194-201.

[5] A. Spek, *Acta Crystallogr., Sect. D: Biol. Crystallogr*, 2009, **65**, 148-155.